

Motion Code: Robust Time Series Classification and Forecasting via Sparse Variational Multi-Stochastic Processes Learning

Chandrajit Bajaj^{1,3} and Minh Nguyen^{2,3}

¹ Department of Computer Science
The University of Texas at Austin

² Department of Mathematics
The University of Texas at Austin

³ Oden Institute for Computational Engineering and Sciences
The University of Texas at Austin

Abstract. Despite being extensively studied, time series classification and forecasting on noisy data remain highly difficult. The main challenges lie in finding suitable mathematical concepts to describe time series and effectively separating noise from the true signals. Instead of treating time series as a static vector or a data sequence as often seen in previous methods, we introduce a novel framework that considers each time series, not necessarily of fixed length, as a sample realization of a continuous-time stochastic process. Such mathematical model explicitly captures the data dependence across several timestamps and detects the hidden time-dependent signals from noise. However, since the underlying data is often composed of several distinct dynamics, modeling using a single stochastic process is not sufficient. To handle such settings, we first assign each dynamics a signature vector. We then propose the abstract concept of the most informative timestamps to infer a sparse approximation of the individual dynamics based on their assigned vectors. The final model, referred to as Motion Code, contains parameters that can fully capture different underlying dynamics in an integrated manner. This allows unmixing classification and generation of specific sub-type forecasting simultaneously. Extensive experiments on sensors and devices noisy time series data demonstrate Motion Code’s competitiveness against time series classification and forecasting benchmarks.

1 Introduction

Noisy time series analysis is a fundamental problem that attracts substantial effort from the research community. However, unlike images, videos, text, or tabular data, finding a suitable mathematical concept to represent and study time series is a complicated task. For instance, consider the data consisting of 2 different groups of time series, which have unequal lengths between 80 and 95 data points and receive 2 distinct colors (see Figure 1). Each group corresponds to the audio data of the a particular word’s pronunciation but pronounced by different people with distinct accents. To capture the underlying shape of these time

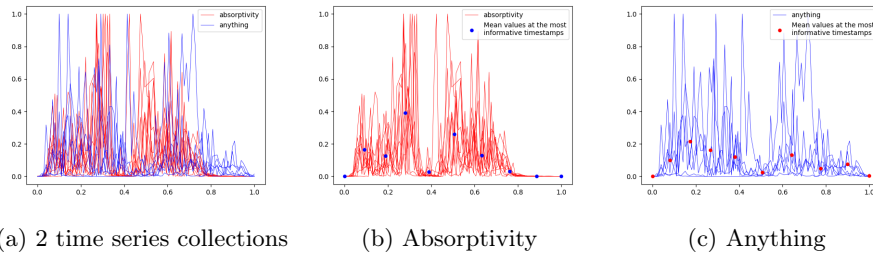


Fig. 1: (a): 2 collections of time series based on pronunciation audio data. Each collection shows the pronunciation of the word **Absorptivity** or **Anything**; (b) and (c): The most informative timestamps for audio data of word **Absorptivity** (red) and word **Anything** (blue).

series, traditional methods view them as ordered vectors and leverage techniques such as distance-based [11], feature-based [18], or shapelet-based [2]. However, such methods are inadequate, particularly in this example where both groups of time series are highly mixed and the shapes of many red series resemble those in blue color (see Figure 1a). For alternative solutions, several frameworks propose treating time series as sequential data and then utilizing recurrent neural networks like LSTM-FCN [12] or advanced convolutional networks on time series like ROCKET [5]. Unfortunately, with limited data size (about 90 data points in this case), it's particularly challenging for these techniques to learn higher-order correlations between several timestamps and capture the exact underlying signals of the time series. Other options like dictionary-based [26], or interval-based [6] methods that rely on empirical statistics gathered along the entire data set are generally unreliable. This is because collected statistics can significantly deviate from the truth value due to noise, and thus it limits their ability to separate noise and underlying signals. Such separation ability is extremely crucial for time series data partially corrupted due to broken recording devices, distorted transmissions, or privacy policies. These challenges motivate us to model time series collections and their underlying signals via abstract stochastic processes.

First, we propose viewing each time series as an instance of a common stochastic process governing the dynamic natures of each series group. With this viewpoint, it is possible that at an individual level, the time series instance contains a large amount of noise. However, given our carefully designed method that is suitable for fitting such underlying stochastic process, the truth dynamics can still be recovered from these noisy instances. For example, the scatter points in Figure 1b and Figure 1c show the skeleton approximations learned via our model for the underlying stochastic processes. While the original dataset is mixed, each skeleton approximation uncovers a hidden common feature between the time series of the same group. In fact, every global movement including going up or down, sharply increasing or decreasing, or staying still, is precisely observed by those

approximations. Because of the generalization level of stochastic process, the learned model not only records the core signals but also yields relevant statistical dependence between multiple data points.

The stochastic viewpoint is not yet sufficient for data composed of multiple underlying dynamical models. Many research works [24,7,3,23] use different types of stochastic processes to model time series. Nonetheless, their approaches are limited within one single dynamical model and often focus solely on one single series. On the other hand, our framework is capable of handling multiple time series by introducing the variational definition of **the most informative timestamps** (see Definition 4). Building upon the stochastic modeling viewpoint, to handle multiple dynamics at once, we assign a signature vector called motion code to each dynamical model and take a joint learning approach to optimize all motion codes together. Augmented by sparse learning techniques, our approach can prevent overfitting for a particular stochastic process and provide enough discrimination to yield distinctive features between individual dynamics.

The final model called **Motion Code** is therefore able to learn across many underlying processes in a holistic and robust manner. Additionally, thanks to stochastic process modeling, Motion Code can provide interpretable dynamics features and handle missing and varying-length time series. To summarize, our contributions include:

1. A learning model called **Motion Code** that jointly learns across different collections of noisy time series data. **Motion Code** explicitly models the underlying stochastic process and is capable of capturing and separating noise from the core signals.
2. **Motion Code** allows solving time series classification and forecasting simultaneously without the need for separate models for each task.
3. An interpretable feature for a collection of noisy time series called **the most informative timestamps** that utilizes variational inference to learn the underlying stochastic process from the given data collection.

1.1 Related works

Time series classification. For time series classification, there are a variety of classical techniques including: distance-based [11], interval-based [6], dictionary-based [26], shapelet-based [2], feature-based [18], as well as ensemble models [14,22] that combine individual classifiers. In terms of deep learning [10], there are convolutional neural network [12,5], modified versions of residual networks [19], and auto-encoders [9].

Time series forecasting For forecasting, researchers have developed several approaches such as exponential smoothing [8], TBATS [4], ARIMA [20], probabilistic state-space models [7], and deep learning frameworks [13,16].

Stochastic modeling of time-series. Gaussian process [25] has been frequently used to model continuous-time series. To reduce the computational cost, sparse Gaussian process [29] has been proposed to approximate the true posterior with pseudo-training examples. Along this line of work, several different versions of generative models together with approximate/exact inference [24,3,23] have been developed. While these works are restricted within one single series, our learning approach applies to generalized multi-time series collections.

The rest of the paper is organized as follows: Section 2 provides mathematical and algorithmic details for our Motion Code framework. Section 3 includes experiments and benchmarkings for Motion Code on time series classification and forecasting. Section 4 presents a discussion advocating the **benefits** of our learning framework.

2 Motion Code: Joint learning on collection of time series

2.1 Problem statement

We first formulate time series problem via stochastic processes context.

Input: Training time series data consist of samples that belong to exactly L ($L \in \mathbb{N} \geq 2$) underlying stochastic processes $\{G_k\}_{k=1}^L$. More specifically, for each $k \in \overline{1, L}$, let $\mathcal{C}_k = \{y^{i,k}\}_{i=1}^{B_k}$ be the sample set consisting of B_k time series $\{y^{i,k}\}_i$, all of which are samples from the k^{th} stochastic process G_k . Here each time series $y^{i,k} = (y_t^{i,k})_{t \in T_{i,k}}$ has the timestamps set $T_{i,k} \subset \mathbb{R}_+$. Each real variable $y_t^{i,k} \in \mathbb{R}$ at time $t \in T_{i,k}$ is called a **data point** of $y^{i,k}$. We also associate the time series $y^{i,k}$ with its data point vector $(y_t^{i,k})_{t \in T_{i,k}} \in \mathbb{R}^{|T_{i,k}|}$. The training data include B collections of time series $\{\mathcal{C}_k\}_{k=1}^B$ corresponding to processes $\{G_k\}_{k=1}^B$.

Tasks and required outputs: The main task is to produce a model \mathcal{M} that jointly learns the processes $\{G_k\}_{k=1}^L$ from the given data $\{\mathcal{C}_k\}_{k=1}^L$. Moreover, the parameters from \mathcal{M} must be learning-transferable to the following tasks:

1. **Classification:** At test time, given a new time series $y = \{y_t\}_{t \in T}$ with timestamps T , classify y into the closest group among L possible groups.
2. **Forecasting:** Suppose a time series y has the underlying stochastic process G_k for a particular $k \in \overline{1, L}$. Given future timestamps T , predict $\{y_t\}_{t \in T}$.

2.2 Three assumptions underlying Motion Code

Motion Code framework models time series via stochastic processes and introduces a novel concept of **the most informative timestamps** to handle multi-time series collections. To simplify mathematical formulation and make explicit computations feasible, we work with a particular type of stochastic processes called nice kernelized Gaussian process (see Definition 1 and Definition 2). The

modeling of this specific stochastic process for Motion Code is expressed through the three assumptions below, which are later used to derive a practical algorithm (Algorithm 1) for noisy datasets.

Definition 1. A stochastic process $G := \{g(t)\}_{t \geq 0}$ is a **kernelized Gaussian process** [25] with the mean function $\mu : \mathbb{R} \rightarrow \mathbb{R}$ and the positive-definite kernel function $K : \mathbb{R} \times \mathbb{R} \rightarrow \mathbb{R}$ iff the joint distribution of the signal vector $g_T = (g(t))_{t \in T}$ on any timestamps set T is Gaussian and is characterized by:

$$p(g_T) = p((g(t))_{t \in T}) = \mathcal{N}(\mu_T, K_{TT}), \quad (1)$$

Here μ_T is the mean vector $(\mu(t))_{t \in T}$, and K_{TT} is the positive-definite $n \times n$ kernel matrix $(K(t, s))_{t, s \in T}$. $\mathcal{N}(\mu, \Sigma)$ denote a Gaussian distribution with mean μ and covariance matrix Σ . The random function g is called **the underlying signal** of the stochastic process G .

Notation: Throughout this paper, for ordered sets T and S of timestamps, we use notation g_T for the signal vector $(g(t))_{t \in T} \in \mathbb{R}^{|T|}$, μ_T for the mean vector $(\mu(t))_{t \in T} \in \mathbb{R}^{|T|}$, and K_{TS} for the $|T|$ -by- $|S|$ kernel matrix $(K(t, s))_{t \in T, s \in S}$.

Definition 2. (Nice Gaussian process) A kernelized Gaussian process $G = \{g(t)\}_{t \geq 0}$ with signal g , kernel K , and mean μ is **nice** if for any two disjoint timestamps sets T and S , the corresponding mean vectors are approximately proportional: $\mu_T \approx K_{TS}K_{SS}^{-1}\mu_S$. In such cases, the conditional distribution of g_T given g_S is Gaussian with the following mean and variance:

$$p(g_T | g_S, T, S) = \mathcal{N}(K_{TS}K_{SS}^{-1}g_S, K_{TT} - K_{TS}K_{SS}^{-1}K_{ST}) \quad (2)$$

Assumption 1: We explicitly model each underlying stochastic process G_k by a kernelized Gaussian process (see Definition 1).

Assumption 2: For $k \in \overline{1, L}$, assume that the data $(y^{i,k})_{t \in T_{i,k}}$ has the Gaussian distribution with mean $(g_k)_{T_{i,k}} = ((g_k)_t)_{t \in T_{i,k}} \in \mathbb{R}^{|T_{i,k}|}$ and covariance matrix $\sigma I_{|T_{i,k}|}$. Here, I_n is the $n \times n$ identity matrix, and g_k is the underlying signal of the stochastic process G_k . Moreover, the constant $\sigma \in \mathbb{R}_+$ is the noise variance of sample data from the underlying signals.

Assumption 3: Assume that G_k is **nice** (see Definition 2) so that the conditional distribution of signal vectors can be simplified to Equation (2).

2.3 The most informative timestamps

In this section, we develop the core mathematical concept behind Motion Code called **the most informative timestamps**. The most informative timestamps of a time series collection generalize the concept of **inducing points** of a single time series that is introduced in [29]. They are a small subset of timestamps that minimizes the mismatch between the original data and the information

reconstructed using only this subset. The visualization of the most informative timestamps is provided in Figure 2 and is further discussed in Section 3.

To concretely define the most informative timestamps, we first introduce **generalized evidence lower bound function** (GELB) in Definition 3. We then define **the most informative timestamps** as the **maximizers** of this GELB function in Definition 4. Finally, assumptions from Section 2.2 allow simplifying the calculation of the **the most informative timestamps** with a concrete formula shown in Lemma 1.

Definition 3. *Suppose we are given a stochastic process $G = \{g(t)\}_{t \geq 0}$ and a collection of time series $\mathcal{C} = \{y^i\}_{i=1}^B$ consisting of B independent time series y^i sampled from G . Each series $y^i = (y_t^i)_{t \in T_i}$ consists of $N_i = |T_i|$ data points and is called a **realization** of G . Let m be a fixed positive integer. We define the **generalized evidence lower bound function** $\mathcal{L} = \mathcal{L}(\mathcal{C}, G, S^m, \phi)$ as a function of the data collection \mathcal{C} , the stochastic process G , the m -elements timestamps set $S^m = \{s_1, \dots, s_m\} \subset \mathbb{R}_+$, and a variational distribution ϕ on \mathbb{R}^m :*

$$\mathcal{L}(\mathcal{C}, G, S^m, \phi) := \frac{1}{B} \sum_{i=1}^B \int p(g_{T_i} | g_{S^m}) \phi(g_{S^m}) \log \frac{p(y^i | g_{T_i}) p(g_{S^m})}{\phi(g_{S^m})} dg_{T_i} dg_{S^m} \quad (3)$$

Again, the vectors g_{T_i} and g_{S^m} are the signal vectors $(g(t))_{t \in T_i} \in \mathbb{R}^{|T_i|}$ and $(g(t))_{t \in S^m} \in \mathbb{R}^{|S^m|}$ on timestamps T_i of y^i and on S^m .

Definition 4. *For a fixed $m \in \mathbb{N}$, the m -elements set $(S^m)^* \subset \mathbb{R}^+$ is said to be **the most informative timestamps** with respect to a noisy time series collection \mathcal{C} of a stochastic process G if there exists a variational distribution ϕ^* on \mathbb{R}^m so that:*

$$(S^m)^*, \phi^* = \arg \max_{S^m, \phi} \mathcal{L}(\mathcal{C}, G, S^m, \phi) \quad (4)$$

Also define the function \mathcal{L}^{max} such that $\mathcal{L}^{max}(\mathcal{C}, G, S^m) := \max_{\phi} \mathcal{L}(\mathcal{C}, G, S^m, \phi)$. Hence, $(S^m)^*$ can be found by maximizing \mathcal{L}^{max} over all possible S^m .

Our Motion Code’s training loss function depends heavily on the function \mathcal{L}^{max} . Lemma 1 below provides a closed-form formula for \mathcal{L}^{max} to help derive the Motion Code’s Algorithm 1.

Lemma 1. *Suppose we’re given a collection \mathcal{C} of B noisy time series $\{y^i\}_{i=1}^B$ sampled from a **nice** Gaussian process $G = \{g(t)\}_{t \geq 0}$ with the underlying signal g . Further assume that the data $(y_i)_{T_i}$ with timestamps T_i has the Gaussian distribution $\mathcal{N}(g_{T_i}, \sigma I_{|T_i|})$ for a given $\sigma > 0$. These assumptions directly follow from Section 2.2 for a single dynamical model with noise variance constant σ .*

Further assume that we’re given a fixed m -elements timestamps set S^m . For $i \in \{1, \dots, B\}$, recall from the notations that $K_{T_i T_i}$, $K_{S^m T_i}$, and $K_{T_i S^m}$ are kernel matrices between timestamps of y^i and S^m . Also define the $|T_i|$ -by- $|T_i|$ matrix

$Q_{T_i T_i} := K_{T_i S^m} (K_{S^m S^m})^{-1} K_{S^m T_i}$ for $i \in \overline{1, B}$. Hence, across all time series, we have the following data vector Y and the joint matrix $Q^{C, G}$:

$$Y = \begin{bmatrix} y^1 \\ \vdots \\ y^B \end{bmatrix}, \quad Q^{C, G} = \begin{bmatrix} Q_{T_1 T_1} & 0 & 0 \\ 0 & \ddots & 0 \\ 0 & 0 & Q_{T_B T_B} \end{bmatrix} \quad (5)$$

Then the function \mathcal{L}^{max} defined in Definition 4 has the following closed-form:

$$\mathcal{L}^{max}(C, G, S^m) = \log p_{\mathcal{N}}(Y|0, B\sigma^2 I + Q^{C, G}) - \frac{1}{2\sigma^2 B} \sum_{i=1}^B \text{Tr}(K_{T_i T_i} - Q_{T_i T_i}) \quad (6)$$

where $p_{\mathcal{N}}(X|\mu, \Sigma)$ denotes the density function of a Gaussian random variable X with mean μ and covariance matrix Σ . Furthermore, the optimal variational distribution $\phi^* = \arg \max_{\phi} \mathcal{L}(C, G, S^m, \phi)$ is a Gaussian distribution of the form:

$$\phi^*(g_{S^m}) = \mathcal{N} \left(\sigma^{-2} K_{S^m S^m} \Sigma \left(\frac{1}{B} \sum_{i=1}^B K_{S^m T_i} y^i \right), K_{S^m S^m} \Sigma K_{S^m S^m} \right) \quad (7)$$

where $\Sigma = \Lambda^{-1}$ with $\Lambda := K_{S^m S^m} + \frac{\sigma^{-2}}{B} \sum_{i=1}^B K_{S^m T_i} K_{T_i S^m}$.

Proof. The proof is given in the **Supplementary Materials**.

2.4 Motion Code Learning

With the core concept of **the most informative timestamps** outlined in Section 2.3, we can now describe Motion Code learning framework in details:

Model and parameters: Let the k^{th} stochastic process G_k be modeled by a **nice** Gaussian process with kernel function K^{η_k} parameterized by η_k for $k \in \overline{1, L}$. Next, we normalized all timestamps to the interval $[0, 1]$. We choose a fixed $m \in \mathbb{N}$ as the number of the most informative timestamps, and a fixed latent dimension $d \in \mathbb{N}$. We model the most informative timestamps $S^{m, k}$ of the k^{th} stochastic process G_k (with data collection \mathcal{C}_k) jointly for all $k \in \overline{1, L}$ by a common map $\mathcal{G} : \mathbb{R}^d \rightarrow \mathbb{R}^m$. More concretely, choose L different d -dimensional vectors $z_1, \dots, z_L \in \mathbb{R}^d$ called **motion codes**, and model $S^{m, k}$ by:

$$\widehat{S^{m, k}} := \sigma(\mathcal{G}(z_k)) \in \mathbb{R}^m, \text{ where } \sigma \text{ is the standard sigmoid function.} \quad (8)$$

We approximate \mathcal{G} by a linear map specified by the parameter matrix Θ so that $\mathcal{G}(z_k) \approx \Theta z_k$. Hence, Motion Code includes 3 types of parameters:

1. Kernel parameters $\eta := (\eta_1, \dots, \eta_L)$ for underlying Gaussian process G_k .
2. Motion codes $z := (z_1, \dots, z_L)$ with $z_i \in \mathbb{R}^d$.
3. The joint map parameter Θ with dimension $m \times d$.

Training loss function: The goal is to make $\widehat{S}^{m,k}$ approximate the true $S^{m,k}$, which is the maximizer of \mathcal{L}^{max} with an explicit formula given in Equation (6). As a result, we want to maximize $\mathcal{L}^{max}(\mathcal{C}_k, G_k, \widehat{S}^{m,k})$ for all k , leading to the following loss function:

$$\mathcal{U}(\eta, z, \Theta) = - \sum_{k=1}^L \mathcal{L}^{max}(\mathcal{C}_k, G_k, \widehat{S}^{m,k}) + \lambda \sum_{k=1}^L \|z_k\|_2^2 \quad (9)$$

Here the last term is the regularization term for the motion codes z_k with hyperparameter λ . An explicit training algorithm is given below (see Algorithm 1).

Algorithm 1 Motion Code training algorithm

Input: L collections of time series data $\mathcal{C}_k = \{y^{i,k}\}_{i=1}^{B_k}$, where the series $y^{i,k}$ has timestamps $T_{i,k}$. Additional hyperparameters include the number of most informative timestamps m , motion codes dimension d , max iteration M , and stopping threshold ϵ .
Output: Parameters η, z, Θ described above that optimize loss function $\mathcal{U}(\eta, z, \Theta)$.

- 1: Initialize η and z to be constant vectors 1, and Θ to be the constant matrix, where each column is the arithmetic sequence between 0.1 and 0.9.
 - 2: **repeat**
 - 3: Use the current parameter η, z to calculate the predicted most informative timestamps for the k^{th} stochastic process: $\widehat{S}^{m,k} = \sigma(\Theta z_k)$.
 - 4: For $k \in \overline{1, L}, i \in \overline{1, B_k}$, calculate $K_{S^{m,k} S^{m,k}}^{\eta_k}, K_{S^{m,k} T_{i,k}}^{\eta_k}, K_{T_{i,k} S^{m,k}}^{\eta_k}$, and the corresponding matrix Q 's, and $Q^{C,G}$ defined in Lemma 1.
 - 5: Use above results to calculate $\mathcal{L}^{max}(\mathcal{C}_k, G_k, \widehat{S}^{m,k})$ given by Equation (6) via an automatic differentiation framework for $k \in \overline{1, L}$.
 - 6: Calculate the loss $\mathcal{U}(\eta, z, \Theta)$ and its differential via automatic differentiation.
 - 7: Update parameters (η, z, Θ) using Limited-memory Broyden Fletcher Goldfarb Shanno (L-BFGS) algorithm [15].
 - 8: **until** numbers of iterations exceed M or training loss decreases less than ϵ .
 - 9: Output the final (η, z, Θ) .
-

2.5 Classification and Forecasting with Motion Code

We use the trained parameters η, z, θ from Algorithm 1 to perform time series forecasting and classification. We need an immediate step of finding **preliminary predictions** that give us the predicted mean signal $p_k = \mathbb{E}[(g_k)_T] \in \mathbb{R}^{|T|}$. With such p_k , we can then perform forecasting and classification tasks.

Preliminary predictions: For a given $k \in \overline{1, L}$, the predicted distribution of the signal vector $(g_k)_T$ is calculated by marginalizing over the signal $(g_k)_{S^{m,k}}$

on the most informative timestamps $S^{m,k}$ of process G_k :

$$p((g_k)_T) = \int p((g_k)_T | (g_k)_{S^{m,k}}) \phi^*((g_k)_{S^{m,k}}) d(g_k)_{S^{m,k}} \quad (10)$$

where the optimal variational distribution ϕ^* is a Gaussian distribution has the following mean μ_k and covariance matrix A_k (based on Lemma 1):

$$\mu_k = \sigma^{-2} K_{S^{m,k} S^{m,k}}^{\eta_k} \Sigma \left(\frac{1}{B_k} \sum_{i=1}^{B_k} K_{S^{m,k} T_{i,k}}^{\eta_k} y^i \right), \quad A_k = K_{S^{m,k} S^{m,k}}^{\eta_k} \Sigma K_{S^{m,k} S^{m,k}}^{\eta_k} \quad (11)$$

where $\Sigma = \Lambda^{-1}$ with $\Lambda := K_{S^{m,k} S^{m,k}}^{\eta_k} + \frac{\sigma^{-2}}{B_k} \sum_{i=1}^{B_k} K_{S^{m,k} T_{i,k}}^{\eta_k} K_{T_{i,k} S^{m,k}}^{\eta_k}$.

The convolution in Equation (10) only involves product of two Gaussians and can be calculated explicitly as:

$$p((g_k)_T) = \mathcal{N}(K_{T S^{m,k}}^{\eta_k} (K_{S^{m,k} S^{m,k}}^{\eta_k})^{-1} \mu_k, K_{TT}^{\eta_k} - K_{T S^{m,k}}^{\eta_k} (K_{S^{m,k} S^{m,k}}^{\eta_k})^{-1} K_{S^{m,k} T}^{\eta_k} + K_{T S^{m,k}}^{\eta_k} (K_{S^{m,k} S^{m,k}}^{\eta_k})^{-1} A_k (K_{S^{m,k} S^{m,k}}^{\eta_k})^{-1} K_{S^{m,k} T}^{\eta_k}) \quad (12)$$

Forecasting: For the stochastic process G_k , we output the mean vector $p_k = \mathbb{E}[(g_k)_T] \in \mathbb{R}^{|T|}$ obtained from Equation (12) as the whole process's prediction.

Classification: To classify a series y with timestamps T , we first calculate $p_k = \mathbb{E}[(g_k)_T] \in \mathbb{R}^{|T|}$ on T from Equation (12) for each $k \in \overline{1, L}$. **Motion Code** outputs a prediction based on the label of the closest p_k :

$$k_{\text{predicted}} = \arg \max_k \|y - p_k\|_{2, \mathbb{R}^{|T|}} \quad (13)$$

Here we use the simple Euclidean distance $\|\cdot\|_{2, \mathbb{R}^{|T|}}$.

Time complexity: The matrix multiplication between matrices of size m -by- m and size m -by- $|T_{i,k}|$ or $|T_{i,k}|$ -by- m is the most expensive individual operation in Algorithm 1. Hence, Algorithm 1 has time complexity $O\left(\sum_{k=1}^L \sum_{i=1}^{B_k} m^2 |T_{i,k}|\right) \times M = O(m^2 N M)$, where $N = \sum_{k=1}^L \sum_{i=1}^{B_k} |T_{i,k}|$ is the total number of data points, M is the max number of iterations, and m is the number of the most informative timestamps. For time series tasks, by the same argument, the cost for predicting a single mean vector p_k defined above is $O(m^2 |T|)$. Hence, the cost for forecasting on timestamps T is $O(m^2 |T|)$. For classification on L groups of time series, classifying a time series with timestamps T is $O(m^2 |T| |L|)$. As m is chosen relatively small, the above complexities are approximately linear with respect to the number of data points of the time series input.

Kernel choice: For implementation, we use spectral kernel of the form $K^\eta(t, s) := \sum_{j=1}^J \alpha_j \exp(-0.5 \beta_j |t - s|^2)$ for parameters $\eta = (\alpha_1, \dots, \alpha_J, \beta_1, \dots, \beta_J)$.

Hyperparameters: In Section 3, we choose the number of the most informative timestamps $m = 10$, the latent dimension $d = 2$, and the number of kernel components $J = 1$. Other hyperparameters include $\lambda = 1$, $\epsilon = 10^{-5}$, $M = 10$.

3 Experiments

Table 1: Classification accuracy (in percentage) table for 7 time series classification algorithms: DTW, TSF, RISE, BOSS, BOSS-E, catch22, and our Motion Code. Values shown are classification accuracies in percentage.

Data sets	DTW	TSF	RISE	BOSS	BOSS-E	catch22	Motion Code
Chinatown	54.23	61.22	65.6	47.81	41.69	55.39	66.47
ECGFiveDays	54.47	58.07	59.35	50.06	58.42	52.85	66.55
FreezerSmallTrain	52.42	54.28	53.79	50	50.95	53.58	70.25
GunPointOldVersusYoung	92.7	99.05	98.73	87.62	93.33	98.41	91.11
HouseTwenty	57.98	57.14	42.02	52.1	57.98	45.38	70.59
InsectEPGRegularTrain	100	100	83.13	99.2	91.97	95.98	100
ItalyPowerDemand	57.05	68.71	65.79	52.77	53.26	55.88	72.5
Lightning7	21.92	28.77	26.03	12.33	28.77	24.66	31.51
MoteStrain	56.47	61.1	61.5	53.83	53.51	57.19	72.68
PowerCons	78.33	92.22	85.56	65.56	77.22	80	92.78
SonyAIBORobotSurface2	63.27	67.68	69.78	48.06	61.91	64.43	75.97
Sound	50	87.5	62.5	68.75	62.5	50	87.5
SineCurves	100	100	100	62.71	100	100	100
UWaveGestureLibraryAll	78.25	83.67	79.79	12.23	74.87	47.38	80.18

3.1 Data sets

We acquire 12 **sensors and devices** time series data sets from publicly available UCR data sets [1]. We prepare 2 additional data sets named **Sound** [21] and **SineCurves**. Each data set consists of multiple collections of time series, and each collection has an unique label. For each of 14 data sets, we add a Gaussian noise with standard deviation $\sigma = 0.3 * A$, where A is the maximum possible absolute value of all data points. The inherent noise in the original data sets is not adequate for robust testing since even simpler algorithms like **DTW** perform very well (achieve near or over 90% accuracy) on many datasets. The noise added thus serves as an adversarial factor to stress test the robustness of time series algorithms. We then implement **Motion Code** algorithm on these 14 datasets to extract optimal parameters for downstream tasks including classification and forecasting. All experiments are executed on Nvidia A100 GPU.

Table 2: Classification accuracy (in percentage) table for 7 time series classification algorithms: Shapelet, Teaser, SVC, LSTM-FCN, Rocket, Hive-Cote 2, and our Motion Code. Values shown are classification accuracies in percentage. Error means running on a given data set has failed.

Data sets	Shapelet	Teaser	SVC	LSTM-FCN	Rocket	Hive-Cote 2	Motion Code
Chinatown	61.22	Error	56.27	66.47	62.97	61.52	66.47
ECGFiveDays	52.61	Error	49.71	53.54	56.79	55.75	66.55
FreezerSmallTrain	50	50.11	50	50	52.67	58.18	70.25
GunPointOldVersusYoung	74.6	89.52	52.38	52.38	90.48	98.73	91.11
HouseTwenty	57.14	53.78	45.38	57.98	58.82	59.66	70.59
InsectEPGRegularTrain	44.58	100	85.94	100	46.18	100	100
ItalyPowerDemand	62.49	63.17	49.85	61.61	70.36	72.98	72.5
Lightning7	20.55	21.92	26.03	17.81	27.4	32.88	31.51
MoteStrain	47.76	Error	50.64	56.55	68.85	56.95	72.68
PowerCons	74.44	51.11	77.78	68.33	87.22	90	92.78
SonyAIBORobotSurface2	69.36	68.84	61.7	63.27	74.71	78.49	75.97
Sound	68.75	Error	62.5	56.25	75	75	87.5
SineCurves	100	96.61	67.8	100	100	100	100
UWaveGestureLibraryAll	49.5	26.52	Error	12.67	83.45	78.5	80.18

We compare Motion Code’s performance on time series classification with 12 other algorithms: **DTW** [11], **TSF** [6], **RISE** [14], **BOSS** [26], **BOSS-E** [26], **catch22** [18], **Shapelet** [2], **Teaser** [27], **SVC** [17], **LSTM-FCN** [12], **Rocket** [5], and **Hive-Cote 2** [22]. Their implementations come from the library **sktime** [17]. We use classification accuracy (measured in percentage) for performance comparison. Table 1 and Table 2 show that **Motion Code** outperforms all other algorithms on **9/14** noisy data sets, and performs second-best for other **3/14** data sets, only behind the ensemble model **Hive-Cote 2**. This result demonstrates our method’s robustness when dealing with collections of noisy time series. Unlike other algorithms, **Motion Code** can handle a time series collection with unequal sequence lengths and missing data. However, for comparison purposes, we don’t consider such special data.

3.2 Time series forecasting

For forecasting, each of the 14 data sets is divided into two parts: 80% of the data points go to train set, and the remaining 20% future data points are set aside for testing. For Motion Code, we output a single prediction for all series in the same collection. We choose 5 algorithms to serve as our baselines: **Exponential smoothing** [8], **ARIMA** [20], **State space model** [7], **TBATS** [4], and **Last seen**. **Last seen** is a simple algorithm that uses previous values to predict next time steps. Their implementations are included in **statsmodels** library [28] and **sktime** library [17]. We run 5 baseline algorithms with individual predictions

Table 3: Average root mean-square error (RMSE) table for 6 time series forecasting algorithms: Exponential smoothing, ARIMA, State-space model, Last seen, TBATS, and Motion Code on 14 data sets. Values shown are RMSE between prediction and ground truth time series averaged over the data points.

Data sets	Exp. Smoothing	ARIMA	State space	Last seen	TBATS	Motion Code
Chinatown	Error	1079	775.96	723.1	633.04	518.49
ECGFiveDays	0.34	0.43	1.58	0.19	0.17	0.27
FreezerSmallTrain	0.88	0.58	0.93	0.57	0.56	0.74
GunPointOldVersusYoung	60.38	128.44	59.83	41.51	20.94	417.94
HouseTwenty	1117	3386	730.51	497.3	560.88	648.27
InsectEPGRegularTrain	0.043	0.095	0.25	0.019	0.02	0.048
ItalyPowerDemand	Error	2.02	2.37	1.24	0.96	0.67
Lightning7	1.7	2.85	1.7	1.35	1.35	1.08
MoteStrain	1.11	1.52	1.09	1.01	0.88	0.82
PowerCons	3.38	4.85	4.41	1.77	1.72	1.15
SonyAIBORobotSurface2	2.79	2.01	3.21	1.39	1.52	2.26
Sound	0.087	0.27	0.086	0.1	0.059	0.085
SineCurves	3.5	4.37	3.53	1.53	1.63	1.07
UWaveGestureLibraryAll	4.37	5	4.45	0.98	1.44	0.98

and provide comparison results in Table 3. Even without making individual predictions, Motion Code still surpasses other methods in 7/14 data sets.

4 Discussion on Motion Code’s benefits

Interpretable feature: Despite having several noisy time series that deviate from the common mean, the points at most informative timestamps $S^{m,k}$ form a skeleton approximation of the underlying stochastic process. All the important twists and turns are constantly observed by the corresponding points at important timestamps (See Figure 2). Those points create a feature that helps visualize the underlying dynamics with explicit global behaviors such as increasing, decreasing, staying still, unlike the original complex time series collections with no visible common patterns among series.

Uneven length and missing data handling: For each time series, Motion Code processes individual data points and their timestamps one by one. Hence, time series fed into the algorithm can have different timestamps sets. We include an experiment to illustrate that even with missing data, Motion Code still learns the underlying dynamics sufficiently well. In the **Sound** data, we remove randomly from each series about 10% of its data points, and retrain the model on the modified data. The time series in the new dataset have both different

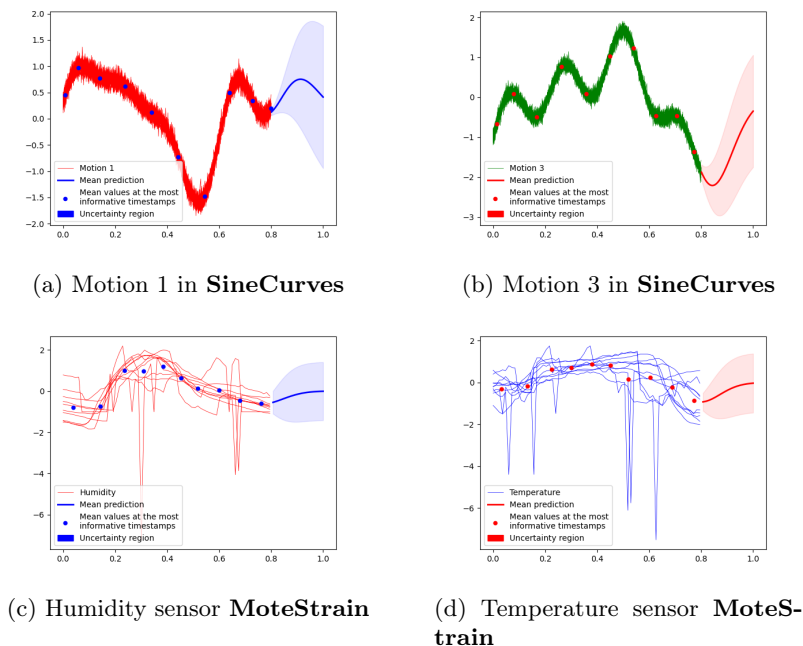


Fig. 2: Forecasting with uncertainty for time series collections in **SineCurves** and **MoteStrain**. Mean values on most informative timestamps are included. Here, we train **Motion Code** on time horizon $[0, 0.8]$ and predict on $[0.8, 1]$.

lengths and out-of-sync timestamps values. The resulting model still gives the same accuracy and accurate skeleton approximation (see Figure 1), showing **Motion Code**'s effectiveness for uneven length and missing data.

Learning effectiveness across multiple time series: To illustrate **Motion Code**'s learning ability across several time series, we compare its performance with an alternative approach which learns from each individual series through a two-step feature extraction procedure on **SineCurves** data. First, we implement sparse Gaussian regression [29] to extract the optimal inducing points from each series and stack them into vector X . Then, we use singular value decomposition to perform the low-rank compression on X and obtain corresponding 2D features. Figure 3 shows that features extracted from this process yield intertwined and inseparable clusters. Additionally, the expensive operations on each individual series are prohibitive in practice. On the other hand, **Motion Code** achieves 100% accuracy (see Table 1) for classification task on the same data set, suggesting the advantage of **Motion Code**'s holistic approach across series and hidden dynamics.

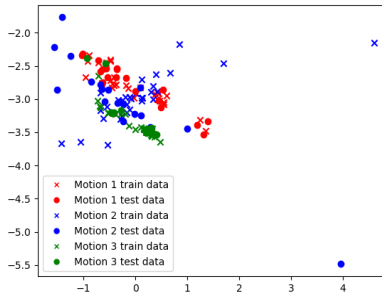


Fig. 3: Two-dimensional features extracted from individual time series in the data set **SineCurves** via separate sparse Gaussian process models.

5 Conclusion

In this work, we employ variational inference and sparse stochastic process model to develop an integrated framework called **Motion Code**. The method can perform time series forecasting simultaneously with classification across different collections of time series data, while most other current methods only focus on one task at a time. Our **Motion Code** model is particularly robust to noise and produces competitive performance against other popular time series classification and forecasting algorithms. Moreover, as we have demonstrated in Section 4, **Motion Code** provides an interpretable feature that effectively captures the core information of the underlying stochastic process. Finally, our method can deal with varying-length time series and missing data, while many other methods fail to do so. In future work, we plan to generalize **Motion Code**, with non-Gaussian priors adapted to time series from various application domains.

Author acknowledgement: This research was supported in part by a grant from the NIH DK129979, in part from the Peter O’Donnell Foundation, the Michael J. Fox Foundation, Jim Holland-Backcountry Foundation, and in part from a grant from the Army Research Office accomplished under Cooperative Agreement Number W911NF-19-2-0333.

Author Contributions: Motion Code is developed by Minh Nguyen and improved by Chandrajit Bajaj and Minh Nguyen. Alphabetical order is currently used to order author names. The implementation is done by Minh Nguyen and is available at https://github.com/mpnguyen2/motion_code.

References

1. Bagnall, A., Lines, J., Bostrom, A., Large, J., Keogh, E.: The great time series classification bake off: a review and experimental evaluation of recent algorithmic advances. *Data Min. Knowl. Discov.* **31**(3), 606–660 (2017)

2. Bostrom, A., Bagnall, A.: Binary shapelet transform for multiclass time series classification. In: Transactions on Large-Scale Data- and Knowledge-Centered Systems XXXII, pp. 24–46. Springer Berlin Heidelberg, Berlin, Heidelberg (2017)
3. Cao, Y., Brubaker, M.A., Fleet, D.J., Hertzmann, A.: Efficient optimization for sparse gaussian process regression. In: Advances in Neural Information Processing Systems. vol. 26. Curran Associates, Inc. (2013)
4. De Livera, A.M., Hyndman, R.J., Snyder, R.D.: Forecasting time series with complex seasonal patterns using exponential smoothing. *J. Am. Stat. Assoc.* **106**(496), 1513–1527 (2011)
5. Dempster, A., Petitjean, F., Webb, G.I.: ROCKET: exceptionally fast and accurate time series classification using random convolutional kernels. *Data Min. Knowl. Discov.* **34**(5), 1454–1495 (2020)
6. Deng, H., Runger, G., Tuv, E., Vladimir, M.: A time series forest for classification and feature extraction. *Inf. Sci. (Ny)* **239**, 142–153 (2013)
7. Durbin, J.: Time Series Analysis by State Space Methods: Second Edition. Oxford University Press (2012)
8. Holt, C.C.: Forecasting seasonals and trends by exponentially weighted moving averages. *Int. J. Forecast.* **20**(1), 5–10 (2004)
9. Hu, Q., Zhang, R., Zhou, Y.: Transfer learning for short-term wind speed prediction with deep neural networks. *Renew. Energy* **85**, 83–95 (2016)
10. Ismail Fawaz, H., Forestier, G., Weber, J., Idoumghar, L., Muller, P.A.: Deep learning for time series classification: a review. *Data Min. Knowl. Discov.* **33**(4), 917–963 (2019)
11. Jeong, Y.S., Jeong, M.K., Omitaomu, O.A.: Weighted dynamic time warping for time series classification. *Pattern Recognit.* **44**(9), 2231–2240 (2011)
12. Karim, F., Majumdar, S., Darabi, H., Harford, S.: Multivariate LSTM-FCNs for time series classification. *Neural Netw.* **116**, 237–245 (2019)
13. Lim, B., Zohren, S.: Time-series forecasting with deep learning: a survey. *Philos. Trans. A Math. Phys. Eng. Sci.* **379**(2194), 20200209 (2021)
14. Lines, J., Taylor, S., Bagnall, A.: HIVE-COTE: The hierarchical vote collective of transformation-based ensembles for time series classification. In: 2016 IEEE 16th International Conference on Data Mining (ICDM). IEEE (2016)
15. Liu, D.C., Nocedal, J.: On the limited memory BFGS method for large scale optimization. *Math. Program.* **45**(1-3), 503–528 (1989)
16. Liu, Z., Zhu, Z., Gao, J., Xu, C.: Forecast methods for time series data: A survey. *IEEE Access* **9**, 91896–91912 (2021)
17. Löning, M., Bagnall, A., Ganesh, S., Kazakov, V., Lines, J., Király, F.J.: sk-time: A Unified Interface for Machine Learning with Time Series. arXiv e-prints arXiv:1909.07872 (Sep 2019)
18. Lubba, C.H., Sethi, S.S., Knaute, P., Schultz, S.R., Fulcher, B.D., Jones, N.S.: catch22: CAnonical time-series CHaracteristics: Selected through highly comparative time-series analysis. *Data Min. Knowl. Discov.* **33**(6), 1821–1852 (2019)
19. Ma, Q., Shen, L., Chen, W., Wang, J., Wei, J., Yu, Z.: Functional echo state network for time series classification. *Inf. Sci. (Ny)* **373**, 1–20 (2016)
20. Malki, Z., Atlam, E.S., Ewis, A., Dagnew, G., Alzighaibi, A.R., ELmarhomy, G., Elhosseini, M.A., Hassanien, A.E., Gad, I.: ARIMA models for predicting the end of COVID-19 pandemic and the risk of second rebound. *Neural Comput. Appl.* **33**(7), 2929–2948 (2021)
21. Media, F.: Forvo: The pronunciation guide. <http://www.forvo.com/> (2022), accessed: 2022-04-01

22. Middlehurst, M., Large, J., Flynn, M., Lines, J., Bostrom, A., Bagnall, A.: HIVE-COTE 2.0: a new meta ensemble for time series classification. *Mach. Learn.* **110**(11-12), 3211–3243 (2021)
23. Moss, H.B., Ober, S.W., Picheny, V.: Inducing point allocation for sparse gaussian processes in high-throughput bayesian optimisation. In: Proceedings of The 26th International Conference on Artificial Intelligence and Statistics. Proceedings of Machine Learning Research, vol. 206, pp. 5213–5230. PMLR (25–27 Apr 2023)
24. Qi, Y., Abdel-Gawad, A.H., Minka, T.P.: Sparse-posterior gaussian processes for general likelihoods. In: Proceedings of the 26th conference on uncertainty in artificial intelligence. pp. 450–457. Citeseer (2010)
25. Rasmussen, C.E., Williams, C.K.: Gaussian processes for machine learning. MIT Press (2006)
26. Schäfer, P.: The BOSS is concerned with time series classification in the presence of noise. *Data Min. Knowl. Discov.* **29**(6), 1505–1530 (2015)
27. Schäfer, P., Leser, U.: TEASER: early and accurate time series classification. *Data Min. Knowl. Discov.* **34**(5), 1336–1362 (2020)
28. Skipper Seabold, Josef Perktold: Statsmodels: Econometric and Statistical Modeling with Python. In: Proceedings of the 9th Python in Science Conference. pp. 92 – 96 (2010)
29. Titsias, M.: Variational learning of inducing variables in sparse gaussian processes. In: Proceedings of the Twelfth International Conference on Artificial Intelligence and Statistics. Proceedings of Machine Learning Research, vol. 5, pp. 567–574. PMLR, Florida, USA (16–18 Apr 2009)

A Proof of Lemma 1

Lemma 1. *Suppose we're given a collection \mathcal{C} of B noisy time series $\{y^i\}_{i=1}^B$ sampled from a **nice** Gaussian process $G = \{g(t)\}_{t \geq 0}$ with the underlying signal g . Further assume that the data $(y_i)_{T_i}$ with timestamps T_i has the Gaussian distribution $\mathcal{N}(g_{T_i}, \sigma I_{|T_i|})$ for a given $\sigma > 0$. These assumptions directly follow from Section 2.2 for a single dynamical model with noise variance constant σ .*

Further assume that we're given a fixed m -elements timestamps set S^m . For $i \in \overline{1, B}$, recall from the notations that $K_{T_i T_i}$, $K_{S^m T_i}$, and $K_{T_i S^m}$ are kernel matrices between timestamps of y^i and S^m . Also define the $|T_i|$ -by- $|T_i|$ matrix $Q_{T_i T_i} := K_{T_i S^m} (K_{S^m S^m})^{-1} K_{S^m T_i}$ for $i \in \overline{1, B}$. Hence, across all time series, we have the following data vector Y and the joint matrix $Q^{\mathcal{C}, G}$:

$$Y = \begin{bmatrix} y^1 \\ \vdots \\ y^B \end{bmatrix}, \quad Q^{\mathcal{C}, G} = \begin{bmatrix} Q_{T_1 T_1} & 0 & 0 \\ 0 & \ddots & 0 \\ 0 & 0 & Q_{T_B T_B} \end{bmatrix} \quad (5)$$

Then the function \mathcal{L}^{\max} defined in Definition 4 has the following closed-form:

$$\mathcal{L}^{\max}(\mathcal{C}, G, S^m) = \log p_{\mathcal{N}}(Y|0, B\sigma^2 I + Q^{\mathcal{C}, G}) - \frac{1}{2\sigma^2 B} \sum_{i=1}^B \text{Tr}(K_{T_i T_i} - Q_{T_i T_i}) \quad (6)$$

where $p_{\mathcal{N}}(X|\mu, \Sigma)$ denotes the density function of a Gaussian random variable X with mean μ and covariance matrix Σ . Furthermore, the optimal variational distribution $\phi^* = \arg \max_{\phi} \mathcal{L}(\mathcal{C}, G, S^m, \phi)$ is a Gaussian distribution of the form:

$$\phi^*(g_{S^m}) = \mathcal{N}\left(\sigma^{-2} K_{S^m S^m} \Sigma \left(\frac{1}{B} \sum_{i=1}^B K_{S^m T_i} y^i\right), K_{S^m S^m} \Sigma K_{S^m S^m}\right) \quad (7)$$

where $\Sigma = \Lambda^{-1}$ with $\Lambda := K_{S^m S^m} + \frac{\sigma^{-2}}{B} \sum_{i=1}^B K_{S^m T_i} K_{T_i S^m}$.

Proof. Define the conditional mean signal vector $\alpha_i = \mathbb{E}[g_{T_i} | g_{S^m}]$. From Equation (2), $\alpha_i = K_{T_i S^m} (K_{S^m S^m})^{-1} g_{S^m}$. Let A be the combined mean signal vector

$A := \begin{bmatrix} \alpha_1 \\ \vdots \\ \alpha_B \end{bmatrix}$. With these notations, following the derivation from [29], individual

terms in Equation (3) can be simplified as follows:

$$\begin{aligned} & \int p(g_{T_i} | g_{S^m}) \phi(g_{S^m}) \log \frac{p(y^i | g_{T_i}) p(g_{S^m})}{\phi(g_{S^m})} dg_{T_i} dg_{S^m} \\ &= \int \phi(g_{S^m}) \left(\int p(g_{T_i} | g_{S^m}) \log p(y^i | g_{T_i}) dg_{T_i} + \log \frac{p(g_{S^m})}{\phi(g_{S^m})} \right) dg_{S^m} \\ &= \int \phi(g_{S^m}) \left(\log p_{\mathcal{N}}(y^i | \alpha_i, \sigma I_{|T_i|}) - \frac{1}{2\sigma^2} \text{Tr}(K_{T_i T_i} - Q_{T_i T_i}) + \log \frac{p(g_{S^m})}{\phi(g_{S^m})} \right) dg_{S^m} \\ &= \int \phi(g_{S^m}) \log \frac{p_{\mathcal{N}}(y | \alpha_i, \sigma I_{|T_i|}) p(g_{S^m})}{\phi(g_{S^m})} dg_{S^m} - \frac{1}{2\sigma^2} \text{Tr}(K_{T_i T_i} - Q_{T_i T_i}) \end{aligned}$$

Using this equation for individual term, we upper-bound the function $\mathcal{L}(S, G, T^m, \phi)$ (see Equation (3)) as follows:

$$\begin{aligned}
& \mathcal{L}(S, G, T^m, \phi) \\
&= \sum_{i=1}^B \frac{1}{B} \int \phi(g_{S^m}) \log \frac{p_{\mathcal{N}}(y^i | g_{T_i}, \sigma^2 I) p(g_{S^m})}{\phi(g_{S^m})} dg_{S^m} - \frac{1}{2\sigma^2 B} \sum_{i=1}^B \text{Tr}(K_{T_i T_i} - Q_{T_i T_i}) \\
&= \int \phi(g_{S^m}) \log \left(\left(\prod_i p_{\mathcal{N}}(y^i | \alpha_i, \sigma^2 I) \right)^{1/B} \frac{p(g_{S^m})}{\phi(g_{S^m})} \right) dg_{S^m} \\
&\quad - \frac{1}{2\sigma^2 B} \sum_{i=1}^B \text{Tr}(K_{T_i T_i} - Q_{T_i T_i}) \\
&\leq \log \int \left(\prod_{i=1}^B p_{\mathcal{N}}(y^i | \alpha_i, \sigma^2 I) \right)^{1/B} p(g_{S^m}) dg_{S^m} - \frac{1}{2\sigma^2 B} \sum_{i=1}^B \text{Tr}(K_{T_i T_i} - Q_{T_i T_i}) \\
&= \log \int p_{\mathcal{N}}(Y | A, B\sigma^2) p(g_{S^m}) dg_{S^m} - \frac{1}{2\sigma^2 B} \sum_{i=1}^B \text{Tr}(K_{T_i T_i} - Q_{T_i T_i}) \\
&= \log p_{\mathcal{N}}(Y | 0, B\sigma^2 I + Q^{C, G}) - \frac{1}{2\sigma^2 B} \sum_{i=1}^B \text{Tr}(K_{T_i T_i} - Q_{T_i T_i})
\end{aligned}$$

The only inequality for this bound is due to Jensen inequality. This upper-bound no longer depends on the variational distribution ϕ and only depends on the timestamps in S^m . As a result, by definition of \mathcal{L}^{max} , we obtain the Equation (6). Moreover, for this bound, the equality holds when:

$$\begin{aligned}
\phi^*(g_{S^m}) &\propto \prod_{i=1}^B p_{\mathcal{N}}(y^i | \alpha_i, \sigma^2 I)^{1/B} p(g_{S^m}) \\
&\propto \exp \left(\frac{\sigma^{-2}}{B} \sum_{i=1}^B \left((y^i)^T K_{T_i S^m} (K_{S^m S^m})^{-1} g_{S^m} \right) - \frac{1}{2} (g_{S^m})^T \times \right. \\
&\quad \left. \left(\frac{\sigma^{-2}}{B} \sum_{i=1}^B \left((K_{S^m S^m})^{-1} K_{S^m T_i} K_{T_i S^m} (K_{S^m S^m})^{-1} \right) + (K_{S^m S^m})^{-1} \right) \times g_{S^m} \right)
\end{aligned}$$

Hence, ϕ^* is a Gaussian distribution with mean and variance as expected:

$$\phi^*(g_{S^m}) = \mathcal{N} \left(\sigma^{-2} K_{S^m S^m} \Lambda \left(\frac{1}{B} \sum_{j=1}^B K_{S^m T_j} y^j \right), K_{S^m S^m} \Lambda K_{S^m S^m} \right) \quad (14)$$

□

B Further explanations on the generalized evidence lower bound function in Definition 3

For each $i \in \overline{1, B}$, for a single time series y^i , we have the following lower-bound estimate for log-likelihood $\log(y^i)$:

$$\begin{aligned} \log y^i &= \log \int p(y^i | g_{T_i}) p(g_{T_i} | g_{S^m}) p(g_{S^m}) dg_{T_i} dg_{S^m} \\ &\geq \int p(g_{T_i} | g_{S^m}) \phi(g_{S^m}) \log \frac{p(y^i | g_{T_i}) p(g_{S^m})}{\phi(g_{S^m})} dg_{T_i} dg_{S^m} \end{aligned}$$

Adding up inequalities for all time series $\{y^i\}_{i=1}^B$ in the collection \mathcal{C} and then taking the mean, we obtain:

$$\begin{aligned} \frac{1}{B} \log \mathcal{C} &= \frac{1}{B} \log \left(\prod_{i=1}^B y^i \right) = \frac{1}{B} \sum_{i=1}^B \log(y^i) \\ &\geq \frac{1}{B} \sum_{i=1}^B \int p(g_{T_i} | g_{S^m}) \phi(g_{S^m}) \log \frac{p(y^i | g_{T_i}) p(g_{S^m})}{\phi(g_{S^m})} dg_{T_i} dg_{S^m} \end{aligned}$$

The above lower-bound on the log-likelihood of the collection \mathcal{C} coincides with Equation (3).

C Other figures and tables

Dataset	Train	Test	Length	Description
Sound	18	18	100	Amplitude values of the audio datasets for the pronunciations of 2 words with different accents.
SineCurves	30	20	500	Time series generated from 3 different functions with sine and cosine components and the Gaussian noise of variance 0.1.

Table 4: Descriptions of 2 data sets created by authors.

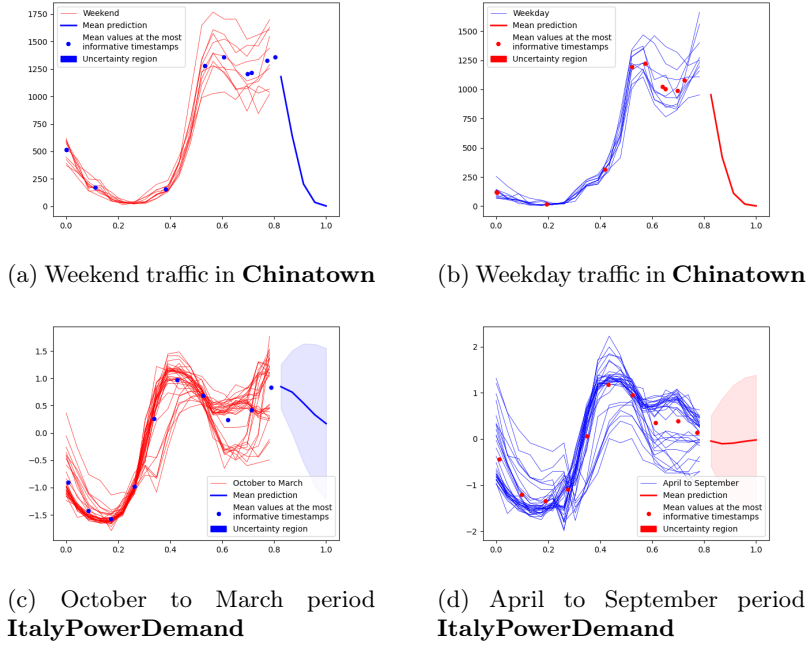


Fig. 4: Forecasting with uncertainty for time series collections in **Chinatown** and **ItalyPowerDemand**. Mean values on most informative timestamps are included. Here, we train **Motion Code** on time horizon $[0, 0.8]$ and predict on $[0.8, 1]$.

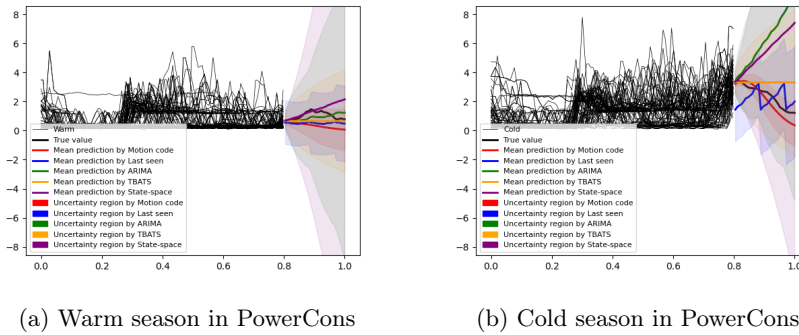


Fig. 5: Forecasting with uncertainty on the **PowerCons** data set from 5 forecasting algorithms: ARIMA, State-space model, Last seen, TBATS, and Motion Code. We train the algorithms on time horizon $[0, 0.8]$ and test on $[0.8, 1]$. **PowerCons** includes two collections of time series: power consumption over the warm and cold seasons. Exponential Smoothing is not included as it doesn't output the uncertainty.